Journal of Electronic Research and Application, 2026, Volume 10, Issue 6
http://ojs.bbwpublisher.com/index.php/JERA
Online ISSN: 2208-3510
Print ISSN: 2208-3502

Structural Design and Optimization of Tesla Valve Based on Bezier Curves

Mingtao Gong*

High School Affiliated to Shanghai Jiao Tong University, Shanghai, China

***Corresponding author:** Mingtao Gong, 770515287@qq.com

Abstract: To reduce forward vortex losses caused by discontinuous curvature in conventional polyline Tesla valves, this study introduces Bezier curves into Tesla valve design to improve unidirectional flow control through curvature continuity. Eight differentiated Bezier-curve configurations (ta-th) are designed, covering concave, convex, and baseline combinations of Curve 1 (inlet to bifurcation midsection) and Curve 2 (bifurcation midsection to outlet). The channel section is set to 3 mm × 2 mm with a bifurcation angle of 20°. A CFD model is established using the standard k-ω turbulence model, with a velocity inlet of 5 m/s and a pressure outlet of 0 Pa gauge to analyze forward and reverse pressure drops, diodicity, and the distributions (pressure, velocity, and turbulent kinetic energy). The results show that the tc structure (concave Curve 1 and convex Curve 2) achieves the best unidirectional flow performance, with a diodicity of 1.700183, a reverse pressure drop of 16035.53 Pa, and a forward pressure drop within 9400–9700 Pa. A concave Curve 1 improves forward flow uniformity and reduces energy loss, whereas a convex Curve 2 strengthens the contraction-expansion effect in reverse flow and enhances blocking capacity. This study confirms that Bezier curves address the structural deficiencies of conventional Tesla valves, establishing links among quantitative geometry, flow, and performance and parametric design rules. This fills a research gap in continuous-curvature structures and provides high-performance passive fluid control for EV thermal management, flame safety, wastewater treatment, as well as theoretical guidance for other passive fluidic devices.

Keywords: Bezier curve; Tesla valve; CFD; Diodicity; Flow-field optimization

Online publication: Jul 23, 2026

1 Introduction

The Tesla valve is a passive unidirectional fluid control device with no moving parts. It was first patented by Tesla, and its diodicity was later experimentally confirmed by Forster et al. [1,2]. The device has a flow diode, with low resistance in the forward direction and high resistance in the reverse direction [3,4]. Due to its simple structure, high reliability, and low maintenance cost, it shows application potential in thermal management, safety protection, ecological engineering, and environmental treatment, and is gradually expanding to new scenarios such as high-pressure differential regulation and system efficiency improvement [5–10]. With the increasing demands on fluid control precision and energy efficiency in modern industry, the traditional polyline Tesla valve is prone to generating local vortices and additional pressure drops due to discontinuous curvature in forward flow, and has problems such as insufficient stability of separation bubbles in reverse flow, limiting its further application [3,11].

Bezier curves have the advantages of continuous curvature, controllable shape, and simple parametric expression, and can achieve smooth flow channel transition through control point adjustment, which helps to reduce forward flow loss and enhance the contraction-expansion effect in reverse flow. Although existing studies have been conducted on bifurcation angles, series, channel widths, and adaptability to multiple scenarios, systematic analysis of continuous curvature structures is still insufficient [3,12–16]. In particular, a unified discussion on the relationship between curve combination morphologies and the pressure, velocity, and turbulent kinetic energy fields is lacking. The unidirectional conduction characteristics of the Tesla valve result from the differential regulation of forward and reverse flow by the flow channel structure [3]. In forward flow, the fluid moves along the main channel attached to the wall, and if the turn is smooth, there will be fewer vortices and lower resistance; in reverse flow, the bifurcation section induces vortices and separation bubbles. Vortices dissipate kinetic energy and separation bubbles occupy the effective channel, thereby significantly increasing flow resistance [2,3,11]. Compared with the traditional polyline structure, the continuous curvature of the Bezier curve mitigates the impact of the forward sharp-angle abrupt change and improves the generation position and stability of the reverse separation bubble.

This study thus designs eight Bezier-curve Tesla valve structures, uses CFD to analyze their pressure drops, diodicity, and flow fields, summarizes optimization rules for curve combinations, and offers a parametric design reference for passive fluidic devices.

2. Characteristics of Tesla valves and theoretical basis of CFD simulation

2.1. Operating principle and key metrics of the Tesla valve

The key performance metrics of a Tesla valve are forward pressure drop ΔPf, reverse pressure drop ΔPr, and diodicity Ri. Here, ΔPf reflects the energy cost of forward transport, ΔPr indicates the flow blocking capability, and a higher diodicity means stronger unidirectional control.

2.2. Technical approach

This study uses Creo for 3D modeling, Ansys Meshing for mesh generation, Ansys Fluent for flow field simulation, and Tecplot for post-processing and visualization.

3. Experimental method and CFD model construction

3.1. Structural design and parameter setting

This paper designs eight different types of Bezier-curve structures (ta-th), including concave, convex, and baseline combinations for Curve 1 (inlet- middle bifurcatcion) and Curve 2 (middle bifurcation - outlet): ta is Curve 1 concave + Curve 2 baseline, tb is Curve 1 concave + Curve 2 concave, tc is Curve 1 concave + Curve 2 convex, td is Curve 1 convex + Curve 2 baseline, te is Curve 1 convex+ Curve 2 concave, tf is Curve 1 convex + Curve 2 convex, tg is Curve 1 baseline + Curve 2 concave, th is Curve 1 baseline + Curve 2 convex. The model uses a 3 mm × 2 mm channel cross-section with a bifurcation Angle of 20° and a single-stage length of approximately 35 mm; continuous control of the channel curvature is achieved by adjusting the coordinates of Bezier control points. Table 1 and 2 present the basic parameters and control point coordinates, respectively.

3.2. Simulation scenarios, boundary conditions, and solver settings

The simulation domain is a single-stage flow channel with equal inlet and outlet lengths. The boundary conditions are set at a velocity inlet of 5 m/s and a pressure outlet of 0 Pa gauge, with a non-slip boundary on the wall. The turbulence intensity is 5%. The solver uses the steady-state pressure-based algorithm, with pressure-velocity coupling handled by the SIMPLEC method. The residual convergence criterion is 1×10^{-5}, and convergence is judged in combination with outlet flow rate and pressure drop variation.

3.3. CFD model construction procedure

Geometric modeling begins with creating a two-dimensional sketch in Creo and drawing the inlet channel. Based on the quadratic Bezier curve formula, the bifurcation start point, end point, and control points are defined. Afterward, the outlet channel and 3D solid model are completed. Then, local refinement is applied to the curved segments and boundary layer regions in Meshing, followed by forward and reverse flow calculations in Fluent (see **Figure 1**).

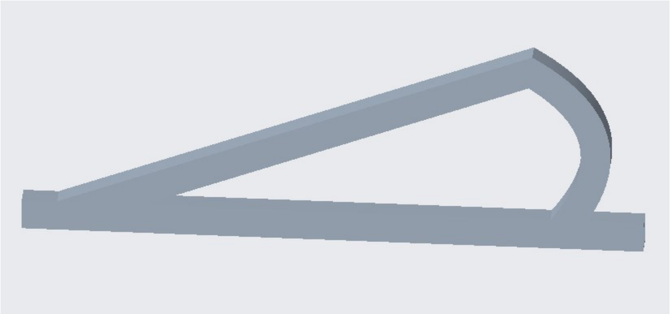

Figure 1. 3D modeling of the Tesla valve.

4. Results and discussions

4.1. Bezier curve analysis of Tesla valve pressure drop and diodicity

To compare the effects of different Bezier-curve structures on the forward and reverse flow performance of Tesla valves, Ansys Fluent is used to simulate the forward pressure drop ΔPf, reverse pressure drop ΔPr, and diodicity Ri of eight structures (ta-th) at flow rates of 0.5–2.0 m/s. The results are shown in **Figure 2**.

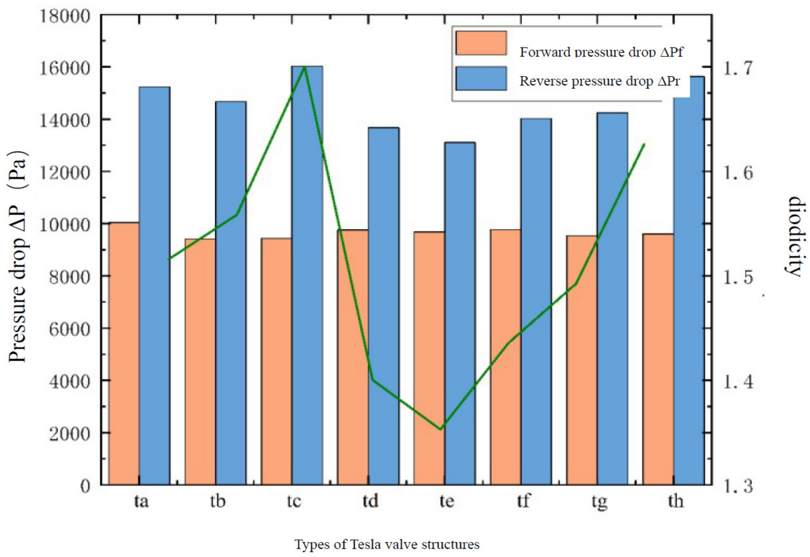

Figure 2. Comparison of Tesla valve performance.

The forward pressure drops of the structures mainly fall between 9400 and 10050 Pa, with little overall difference. Among them, ta has the highest forward pressure drop (10050.32 Pa), while tc, td, and tf are relatively low (about 9400–9700 Pa), indicating that the energy loss in forward flow is similar for most schemes. In scenarios such as thermal management and fluid delivery where forward resistance is emphasized, tc, td, and tf can be prioritized to reduce system energy consumption. The difference in reverse pressure drop is more pronounced, ranging from 13105 to 16035 Pa. tc is the highest (16035.53 Pa), followed by th (15626.48 Pa) and ta (15236.79 Pa), and te is the lowest (13105 Pa). The greater the reverse pressure drop, the stronger the blocking effect of the structure on the reverse fluid. Therefore, tc, th, and ta have an advantage in scenarios that require strong reverse flow blocking, such as fire suppression and wastewater treatment; te, with its lower reverse pressure drop, is more suitable for microfluidic scenarios where the requirements for flow blocking are not high.

The diodicity directly reflects the unidirectional conduction ability of the Tesla valve. The greater the Ri, the better the unidirectionality. tc has the highest diodicity (1.700183), followed by th (1.625938) and tb (1.558484), and te has the lowest (1.353051). This indicates that tc does not significantly increase forward loss while significantly enhancing reverse blocking, and thus achieves the best overall unidirectional conduction performance.

4.2. Bezier curve characteristics of pressure distribution in tesla valve flow field

Based on the Ansys Fluent simulation results, the static pressure nephograms (**Figure 3**) of the ta and td structures under the forward (tal/tdl) and reverse (tar/tdr) conditions are extracted, and the influence of the concave and convex of Curve 1 on the pressure distribution is analyzed.

Figure 3. Diagram of pressure variation affected by Curve 1.

Both structures present the basic feature of high pressure at the inlet and low pressure at the outlet, but the curve shape affects the uniformity of the pressure gradient and local losses. In forward flow, the pressure distribution of ta is relatively uniform, mainly concentrated in the 0–10000 Pa range, with very small local low-pressure areas, indicating that the forward pressure is reduced and the flow is relatively smooth; td, on the other hand, has a local low-pressure area of –5000 to 0 Pa, with slightly poorer pressure uniformity and slightly higher forward pressure drop. The concave curve is more conducive to smooth flow diversion, while the convex curve is more likely to cause local pressure loss. In reverse flow, ta exhibits large high-pressure (15000–20000 Pa) and strong low-pressure (–20000 to –15000 Pa) regions, indicating strong reverse blocking capability and thus a higher diodicity. In contrast, td has a smaller high-pressure region and weaker low-pressure intensity, so its reverse blocking effect is less pronounced than that of ta. Thus, when Curve 1 adopts a concave morphology, it tends to generate a stronger pressure gradient, which favors low forward resistance and high reverse resistance.

As can be seen from **Figure 4**, tg and th have similar pressure distributions in forward flow, both mainly 0–10000 Pa, with little difference in forward flow performance; however, in reverse flow, the range and intensity of the high-pressure zone of th are stronger than those of tg, and the flow-blocking effect is more prominent. Therefore, both tg and th are suitable for the forward low-resistance scenario, while th is more advantageous when a stronger reverse blocking is required.

Figure 4. Diagram of pressure variation affected by Curve 2.

As shown in **Figure 5**, a comparison of tbl, tcl, tel, tfl and their reverse counterparts reveals that in forward flow, tb has the most uniform pressure distribution, and tc, though showing some local low-pressure areas, still performs well overall. Although the pressure gradients of te and tf are relatively gentle, their reverse flow blocking capacity is insufficient. In reverse flow, tc has the largest high-pressure region and the strongest low-pressure region, which corresponds to the highest diodicity, indicating its strongest reverse blocking performance; tb ranks second, but its overall performance is still inferior to that of tc and th; te and tf have weaker high-pressure regions and have poorer blocking performance. Overall, tc performs best in terms of pressure distribution and diodicity, and is more suitable for scenarios that require strong reverse flow blocking, such as fire blocking and wastewater treatment.

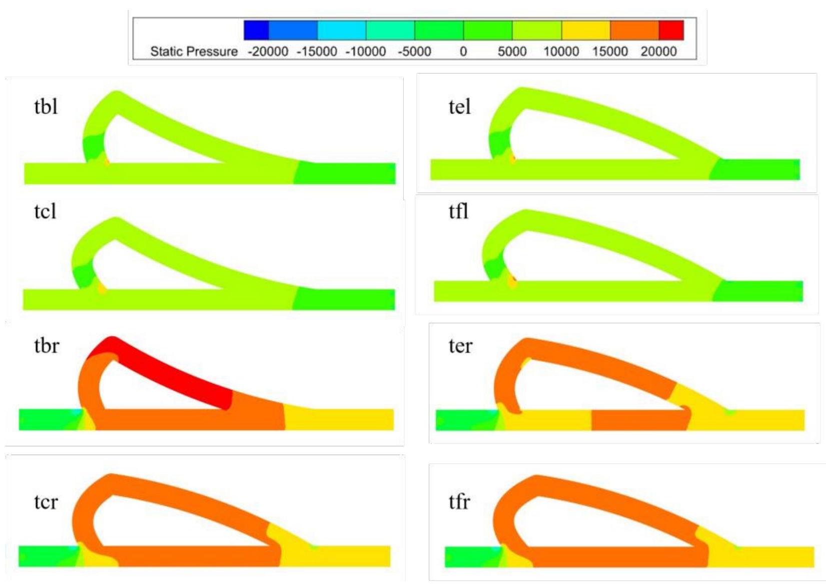

Figure 5. Diagram of the combined effect of Curves 1 and 2 on pressure variation.

4.3. Bezier curve characteristics of velocity distribution in the flow field of Tesla valve

Using the velocity nephograms (**Figure 6**) from Ansys Fluent, the velocity distribution differences between ta and td in forward and reverse flow are analyzed:

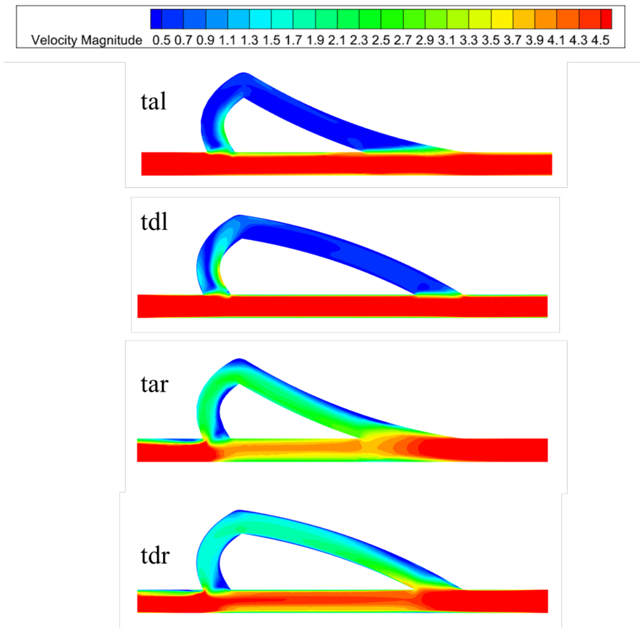

Figure 6. Velocity variation affected by Curve 1.

In forward flow, the mainstream velocity of ta (2.5–3.5 m/s) is uniformly distributed along the flow channel, with a small velocity gradient (≤ 1.0 m/s), and the continuous curvature of the concave curve makes the fluid movement trajectory smooth without obvious velocity change zones, meeting the requirement of uniform flow velocity in thermal management systems; td has a lower mainstream velocity (2.0–3.0 m/s), a velocity change zone (≥ 1.5 m/s) appears at the junction of curve 1 and the bifurcation section, and the convex curve expansion–contraction pattern causes a sudden change in the local channel cross-section, resulting in velocity fluctuations and increased energy dissipation. In reverse flow, the ta bifurcation forms a large high-speed area (3.5–4.5 m/s) with a large velocity gradient (≥ 2.0 m/s). The concave curve guides the reverse fluid to form a stable large-scale vortex where the velocity is low at the center and high at the periphery, thereby enhancing the flow blocking effect. For td, the high-velocity region is smaller (3.0–4.0 m/s), and the velocity gradient is lower than that of ta (≤ 1.5 m/s). The convex curve disperses the reverse fluid, leading to small-scale vortices with poor stability. Thus, its reverse blocking effect is weaker than that of the concave curve.

With Curve 2 unchanged in its baseline morphology, the concave Curve 1 optimizes forward velocity uniformity and enhances reverse velocity gradient, balancing low forward resistance with high reverse resistance; the convex form leads to forward velocity fluctuations and a weaker reverse gradient, with both forward efficiency and reverse resistance being weaker than the concave form. This rule corroborates the pressure distribution analysis. The concave-convex shape of Curve 1 is the core variable for regulating the forward and reverse performance of the Tesla valve. The preference for the concave shape of Curve 1 provides a clear direction for geometric optimization.

Based on the velocity nephogram (**Figure 7**), the velocity distributions of tbl, tcl, tel, tfl, and their reverse structures tbr, tcr, ter, tfr are analyzed.

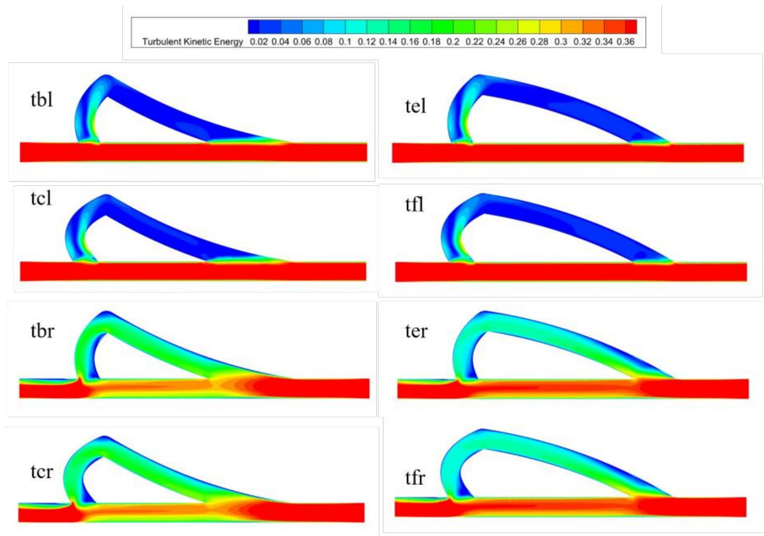

Figure 7. Combined effect of Curve 1 and Curve 2 on velocity variation.

In forward flow, the mainstream velocity of tb is relatively uniform (2.5–3.5 m/s), the velocity gradient is small, and the forward flow efficiency is relatively high, which is basically consistent with its higher diodicity. tc has a slightly higher velocity gradient, but its diodicity indicates that the reverse blocking performance is more prominent, so this part of the forward disadvantage is still acceptable. The velocity distribution of the te and tf structures is relatively stable, but the diodicity is relatively low, indicating insufficient reverse optimization. Overall, the more the channel geometry conforms to the fluid flow path, the more uniform the velocity distribution tends to be. In reverse flow, tc forms a large high-speed region (3.5–4.5 m/s) in the bifurcation section, with the maximum velocity gradient corresponding to its maximum diodicity, indicating that its vortex energy dissipation effect is the strongest. te has a slower velocity gradient and a weaker reverse flow blocking capacity, which is consistent with its lower diodicity. Overall, the reverse velocity characteristics are closely related to the blocking and guiding effects of the structure. The easier it is to form a stable large-scale vortex in the flow channel, the more obvious the velocity gradient and the stronger the reverse blocking ability. The velocity distribution results are largely consistent with the diodicity ranking. tc is the structure with the best unidirectional performance, followed by th and tb.

4.4. Bezier curve characteristics of turbulent kinetic energy distribution of Tesla valve

Based on the turbulent kinetic energy nephogram (**Figure 8**), the turbulent kinetic energy distribution of ta and td in the forward and reverse flow is analyzed under the condition that Curve 2 maintained the baseline morphology to investigate the influence of Curve 1 shape on the turbulent intensity.

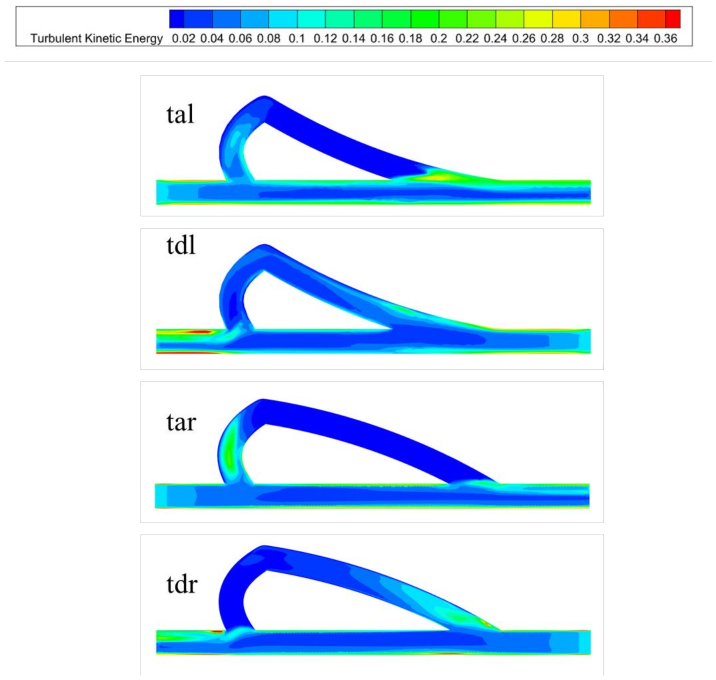

Figure 8. Turbulent kinetic energy affected by Curve 1.

In forward flow, the turbulent kinetic energy of ta is generally low (≤ 0.2). Only at the junction between the bifurcation section and the main channel does a local high-value region (0.2–0.25) appear. This indicates that the concave curve forms a smoother flow-guiding channel. The fluid motion is more stable, and turbulent disturbance is weaker. These observations are consistent with its relatively uniform velocity field and mild pressure gradient. Thus, the concave curve effectively suppresses turbulent dissipation in forward flow. In contrast, td has a larger range of high values of turbulent kinetic energy (0.25–0.3) and a local peak (≥ 0.3) at the root of curve 1, indicating that the abrupt change of cross-section and local vortices caused by the convex curve can enhance the forward turbulent disturbance and increase the energy loss. In reverse flow, ta shows a concentrated and stable high-TKE region (0.25–0.3) in the bifurcation section, indicating that the concave curve more easily induces large-scale stable vortices and sustained turbulent energy concentration. This aligns with the distinct high-velocity gradient and strong low-pressure zone, demonstrating a strong reverse turbulent blocking effect. The high-value area of td is more dispersed and has a lower intensity (0.2–0.25). This indicates that the small-scale vortices induced by the convex curve have poor stability. They can hardly sustain a continuous turbulent energy dissipation process, so the reverse blocking capability of td is weaker than that of ta. Overall, with Curve 2 unchanged, the concave form of Curve 1 can balance forward low dissipation and reverse high blocking, while the convex form can result in greater forward energy loss and weaker reverse blocking effect. This result corroborates the previous analyses of velocity and pressure fields. It indicates that the concave or convex form of Curve 1 is a key factor affecting the turbulent characteristics of the Tesla valve; it is more reasonable to give priority to the concave shape of Curve 1 in scenarios such as thermal management and flame blocking where both forward efficiency and reverse flow blocking are concerned.

Based on the turbulent kinetic energy nephogram (**Figure 9**), the turbulent kinetic energy distributions of tbl, tcl, tel, tfl, and their reverse structures tbr, tcr, ter, tfr are analyzed.

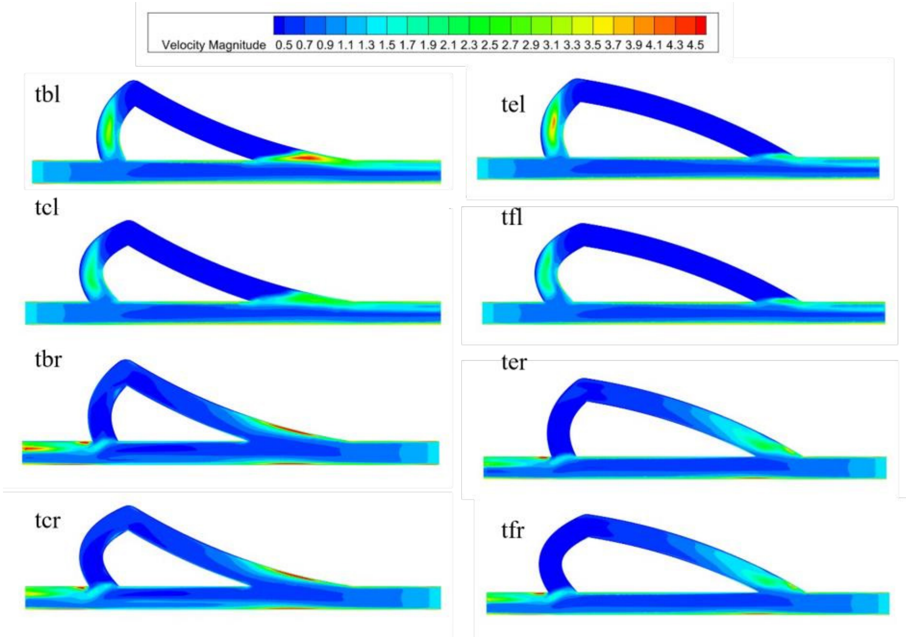

Figure 9. Combined effect of Curves 1 and 2 on turbulent kinetic energy variation.

In forward flow, the turbulent kinetic energy of the tb structure is lower (≤ 0.2), and the local high value area of the bifurcation section is smaller, indicating less forward energy dissipation, which is basically consistent with its higher diodicity. The turbulent kinetic energy of tc is slightly higher, but the conduction ratio indicates that its reverse advantage is sufficient to compensate for the forward loss. The turbulent gradients of the te and tf structures are relatively gentle, but the diodicity is relatively low, and the overall performance is still weak. This indicates that the more the channel geometry fits the fluid motion, the less turbulent dissipation is usually. In reverse flow, the high-value region of turbulent kinetic energy of tc is most concentrated (0.25–0.3), and the distribution is stable, corresponding to the highest diodicity, indicating the strongest turbulent blocking effect; tb has the second-best turbulent kinetic energy, but its overall performance is still inferior to tc; th has a similar turbulent intensity to tb but a higher diodicity; te has weaker turbulent kinetic energy and poorer reverse flow blocking capacity. Overall, the distribution of turbulent kinetic energy is largely consistent with the change in diodicity. tc shows the best combined performance through stronger reverse turbulent energy dissipation, and th and tb can be considered as alternatives.

5. Conclusion

This paper presents a parametric design of the Tesla valve flow channel using Bezier curves and systematically analyzes the flow performance of different structural configurations via CFD. The results show that among the eight Bezier-curve structures, tc (concave Curve 1 and convex Curve 2) has the best overall performance, with a diodicity of 1.700183, a reverse pressure drop of 16035.53 Pa, and a stable forward pressure drop in the range of 9400–9700 Pa. This structure effectively balances low forward resistance with high reverse resistance. Further analysis reveals that the concave form of Curve 1 is conducive to improving the uniformity of the forward flow field and reducing local vortices and energy dissipation; Curve 2, with its convex shape, can enhance the contraction-expansion effect in reverse flow and strengthen the separation and blocking capacity. The research demonstrates that the continuous curvature flow channel design can effectively improve the flow characteristics of the traditional Tesla valve. It provides a theoretical basis for subsequent structural parameter optimization and engineering applications, and offers a reference for improving the design level of passive fluid control devices.

Disclosure statement

The author declares no conflict of interest.

References

[1] Tesla N, 1920, Valvular Conduit. US1329559A.

[2] Forster F, Bardell L, Afromowitz M, et al., 1995, Design, Fabrication and Testing of Fixed-Valve Micro-Pumps. 39–44.

[3] Hu P, 2023, Research on the Diodictiy Characteristics and Its Optimal Design Method of Tesla Valve, thesis, Zhejiang University.

[4] Zhang Z, Chen Z, Chen T, 2020, The Structural Design of Tesla Valves Based on Finite Element Analytical Simulation and 3D Printing Technology. College Physics, 40(4): 73–77.

[5] Zhang W, Guo Y, 2024, Numerical Study on Heat Transfer Characteristics of Tesla Valve-Type Pulsating Heat Pipe. Chemical Engineering, 52(8): 37–42.

[6] Liu X, et al., 2025, Study on Flame Propagation and Quenching Characteristics in Tesla Valve Structure Flame-Retardant Units. Journal of Safety and Environment, 25(5): 1700–1709.

[7] Du P, 2023, Analysis of the Influence of Channel Form and Layout on the Hydraulic Performance of the Emitter, thesis, Taiyuan University of Technology.

[8] Li P, 2024, Numerical Simulation of Hydraulic Cavitation Based on Tesla Valve, thesis, North China Electric Power University (Beijing).

[9] Zhong Z, 2023, Application of the Tesla Valve in Pressure Regulation Under Large-Gradient and High-Pressure-Difference Conditions. Proceedings of the 5th Gas Safety Exchange Seminar, 2: 114–116.

[10] Ren P, Long W, 2021, Numerical Analysis of Flow Field Characteristics and Hydrodynamic Cavitation Mechanism of Tesla Valves. Journal of Southwest University (Natural Science Edition), 43(8): 161–166.

[11] Gamboa A, Morris C, Forster F, 2005, Improvements in Fixed-Valve Micropump Performance Through Shape Optimization of Valves. Journal of Fluids Engineering, 127(2): 339–346.

[12] Su C, et al., 2025, Research on the Influence of Tesla Valve Structural Parameters on One-Direction Flow Characteristic and Modification. Journal of Chemical Engineering of Chinese Universities, 39(6): 993–1001.

[13] Zhou R, et al., 2020, Simulating the Performance of Tesla Valve. Physical Experiment, 40(9): 44–50.

[14] Thompson S, Walters D, Paudel B, et al., 2013, A Numerical Investigation of Multi-Staged Tesla Valves, ASME 2013 Fluids Engineering Division Summer Meeting.

[15] Zhang Y, Tong J, Zhu Z, 2023, Numerical Calculation of Forward and Reverse Flow in Tesla Valves with Different Longitudinal Width-to-Narrow Ratios. Scientific Reports, 13(1): 12496.

[16] Xi C, 2023, Design and Characterization of Tesla Runner With Flow Diodictiy Property and Its Metamaterial Structure, thesis, Yanshan University.